Acta Crystallographica Section B
Structural Science
ISSN 0108-7681

Hydrogen-bonding properties of galanthamine: an investigation through crystallographic database observations and computational chemistry

Soleymane Koné,[a] Nicolas Galland,[a] El-Hadji Sawaliho Bamba[b] and Jean-Yves Le Questel[a]*

[a]Université de Nantes, Nantes Atlantique Universités, Laboratoire de Spectrochimie et Modélisation, EA 1149, FR CNRS 2465, 2 rue de la Houssinière, BP 92208, Nantes F-44000, France, and [b]Université d'Abidjan-Cocody, Laboratoire de Chimie Organique Structurale, UFR SSMT, 22 BP 582, Abidjan 02, Côte d'Ivoire

Correspondence e-mail: jean-yves.le-questel@univ-nantes.fr

Received 21 November 2007
Accepted 14 March 2008

The hydrogen-bonding properties of galanthamine have been investigated experimentally from a thorough analysis of crystallographic data retrieved from the Protein Data Bank and Cambridge Structural Database databases and theoretically through *ab initio* [MP2/6-311++G(2d,p)] and density functional theory [MPWB1K/6-31++G(d,p)] calculations. The main hydrogen-bond acceptor (HBA) interaction sites of the molecule are the O atoms and their spatial proximity allows multi-centered hydrogen-bond (HB) motifs. The hydrogen-bond donor (HBD) sites of the molecule are the NH^+ and OH groups as well as several CH donors. Among them, the preferred ones are those directly linked to the ammonium nitrogen, followed by aromatic CH and finally the methyl group of the methoxy substituent. All these observations are in fairly good agreement with the computed positions of the molecular electrostatic potential (MEP) minima and maxima of various galanthamine species. The galanthamine HBD and HBA properties, investigated through the MEP analysis, appear sensitive to the degree of neutralization of the ammonium NH^+ positive charge.

1. Introduction

Galanthamine (1) (Fig. 1) is an alkaloid found in the bulb and flowers of the common snowdrop (*Galanthus nivalis*) and of several members of the *Amaryllidaceae* family (Proskurnina & Yakovleva, 1952). It has received recent attention as a central nervous system (CNS) acting, selective, competitive and reversible cholinesterase inhibitor that produces significant improvement in the symptomatic treatments of Alzheimer's Disease (AD; Sramek *et al.*, 2000; Weinstock, 1999). Despite a debate on their efficiency, acetylcholinesterase (AChE) inhibitors indeed remain the first and most developed drugs against AD. Commercially available as Reminyl®, Nivalin® and more recently Razadyne®, galanthamine is the most recently approved AChE inhibitor in Europe and USA. Furthermore, galanthamine has recently emerged as a representative member of a new and promising class of anti-Alzheimer agents: it has also been identified as a positive allosteric modulator of nicotinic acetylcholine receptors (nAChR; Lilienfeld, 2002; Santos *et al.*, 2002). Indeed, as the binding site of galanthamine on nAChR should be different to those of nicotinic agonists, secondary effects due to receptor desensitization observed for the nAChRs agonists are expected to be suppressed (Geerts *et al.*, 2002). The importance of galanthamine is assessed by the significant number of related entries in the Cambridge Structural Database (CSD; Allen, 2002). In a recent study devoted to galanthamine structure in its neutral (GAL) and protonated ($GALH^+$) forms, we have found 13 refcodes corresponding to galan-

thamine derivatives (Kone *et al.*, 2006). In the Protein Data Bank (PDB; Berman *et al.*, 2000), five complexes of AChE with galanthamine derivatives are found. These X-ray structure determinations have pointed out the unexpected orientation of the ligand within the active site as well as unusual protein–ligand interactions. Among these interactions, hydrogen bonding has been recognized to play a key role. For example, the cyclohexenol ring hydroxyl group O15H forms a strong HB with the charged Glu199 ($O^{\varepsilon 1}$) and also interacts with conserved water molecules (Greenblatt *et al.*, 1999; Bartolucci *et al.*, 2001). However, a detailed description of ligand–protein interactions requires high-resolution data, below 2.3 Å (Panigrahi & Desiraju, 2007). Furthermore, although X-ray structures of protein–ligand complexes are directly relevant to rational drug design, their precision is not sufficient since, for example, H atoms are almost never located. Finally, molecular docking investigations have been able to predict the bound conformation of galanthamine in the AChE active site, but the docking cannot differentiate between axial and equatorial *N*-methyl conformers (Bartolucci *et al.*, 2001). In the same vein, the putative binding sites of allosteric modulators (including galanthamine) to nAChRs have been recently investigated by a 'blind docking approach' (Iorga *et al.*, 2006). Although docking programs are becoming increasingly sophisticated, their results are strongly dependent of the force field used and their ability to describe properly particular protein–ligand interactions (*e.g.* weak CH$\cdots\pi$ hydrogen bonds).

Despite its importance in the molecular recognition process with AChE, the hydrogen-bonding properties of galanthamine do not appear to have been fully studied so far. To our knowledge, the only exception is the spectroscopic and solid-state study of Carroll and coworkers which was specifically devoted to the hydroxyl group behaviour (Carroll *et al.*, 1990). In this paper we address this issue through an investigation based on solid-state observations (CSD and PDB) and computational chemistry. We have focused on the HB interactions of galanthamine in crystalline environments through:

(i) the associated geometric parameters (distances, linearity and directionality angles) and the nature of the HBDs and HBAs;

(ii) the occurrence of specific motifs (three-centered or bifurcated HB).

From a theoretical point of view, we have first computed the energetic parameters corresponding to the neutralization of protonated galanthamine by several chemical species. A chloride anion is chosen to reach full neutralization and a water or a benzene molecule have been selected to mimic compounds present in the blood or in the AChE active site. Indeed, the comprehensive analysis of Steiner on the water molecules located at the AChE active-site gorge has shown their possible structural and functional importance (Koellner *et al.*, 2000). On the other hand, there is evidence for the implication of several aromatic amino acids (Trp84, Phe331) in the binding to AChE through cation–π interactions with the ammonium group inhibitors (Wlodek *et al.*, 1997). Benzene may mimic the interaction of $GALH^+$ with such aromatic residues. In a second step we have computed the molecular electrostatic potentials (MEP) on the van der Waals surfaces (V_s) of the various $GALH^+X$ ($X = Cl^-$, H_2O, C_6H_6) complexes to probe their respective HB interaction sites. In fact, it has recently been shown that the HB properties of alkaloids of biological interest such as nicotine are strongly dependent on their chemical form (Graton, van Mourik *et al.*, 2003). The V_s minima and maxima allow the localization and the analysis of the preferred HBA and HBD sites, and throw light on the influence of the *X* neutralizing species on these properties.

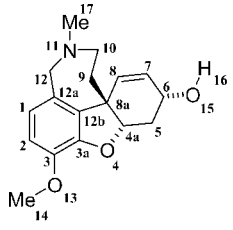

(1)

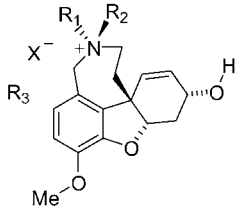

(2) R_1=H, R_2=Me, R_3=Me, X=Br
(3) R_1=R_2=Me, X=I
(4), (5) R_1=Me, R_2=Bu, R_3=H, X=I
(6) R_1=Bu, R_2=Me, R_3=H, X=I
(7) R_1=R_2=R_3=H, X=Cl
(8) R_1=Me, R_2= R_3=H, X=Br
(9) R_1=Me, R_2=CH_2Cl, R_3=H, X=Cl

Figure 1
Structure and numbering of neutral and charged galanthamine derivatives found in the CSD and PDB.

2. Methods

2.1. PDB and CSD searches

The protein–galanthamine complexes were found through a PDB search using the 'galanthamine' keyword. Most of these three-dimensional structures correspond to complexes with AChE. Interactions involving heteroatoms of galanthamine or AChE residues were considered as HB if the distance between the corresponding heavy atoms was less than 3.5 Å. For interactions between C atoms of galanthamine or AChE residues and heteroatoms of the ligand or the protein, a distance criterion of 3.8 Å was used. The geometric parameters corresponding to interactions with aromatic residues were measured with respect to the centroid (Ce) of the aromatic systems. These limits have been applied by Steiner for the analysis of HB interactions in AChE (Koellner *et al.*, 2000, 2002). The environment of galanthamine in AChE has been investigated with the *PyMol* program (Delano, 2004) by selecting any residue within a sphere of 4 Å. The superposition of the AChE binding sites has been made with the *Relibase* program, Version 1.3.2 (Hendlich *et al.*, 2003).

The galanthamine crystallographic data were retrieved from the 2007 release (5.28, 400 977 entries) of the CSD (Allen, 2002). The *ConQuest* program (Bruno *et al.*, 2002) was

used to search for galanthamine substructures and intermolecular non-bonded contacts. Searches were restricted to entries with:

(i) error-free coordinate sets in CSD check procedures;
(ii) no crystallographic disorder;
(iii) no polymeric connections;
(iv) a crystallographic R factor lower than 0.10.

All H atoms involved in non-bonded contact searches were placed in normalized positions (Allen *et al.*, 1987). Non-bonded contact searches and geometrical analysis of HB interactions involving galanthamine HBD and HBA were carried out using the recommendations of Desiraju & Steiner (1999). The HB lengths were respectively expressed from the hydrogen (d) and heavy atom (D) positions of the HBD. To quantify the linearity and directionality of the interactions, we have measured the θ (DH$\cdots A$) and Φ (H$\cdots AY$) HB angles. A contact was accepted as a hydrogen bond only if D was less than 3.8 Å. This criterion allows for the detection of strong to moderate HB (of the type O15H$\cdots A$, with A as the acceptor) and weak ones of the type CH$\cdots A$. The ranges considered for the HB linearity and directionality were $90 \leq \theta\ (\Phi) \leq 180^{\circ}$.

2.2. Theoretical calculations

All the calculations were carried out using the *GAUSSIAN*03 (Frisch *et al.*, 2004) and *Jaguar*6.0 (Schrödinger, 2005) packages. We have selected for our calculations the recent MPWB1K density functional (Zhao & Truhlar, 2004). Indeed, DFT computations remain very appealing owing to their excellent performance-to-cost ratio. Hybrid meta functionals such as MPWB1K have proven to outperform the popular B3LYP functional for non-bonded interactions (Zhao & Truhlar, 2004, 2005*a*,*b*; Zhao *et al.*, 2005). The geometrical structures of the various species were obtained at the MPWB1K/6-31++G(d,p) level of theory. These structures were confirmed as true minima *via* harmonic vibrational frequency calculations. Total energies were then recalculated at the MP2/6-311++G(2d,p) level within the frozen core approximation. For the sake of simplicity, MPWB1K/6-31++G(d,p) and MP2/6-311++G(2d,p)//MPWB1K/6-31++G(d,p) notations will be respectively replaced by MPWB1K and MP2//MPWB1K throughout the text. All presented energies were corrected using unscaled zero-point vibrational energy computed at the MPWB1K level of theory. Optimized geometries of the various species are available as supporting information.[1]

At first we considered the two main minima of GALH$^+$ identified in a recent study (Kone *et al.*, 2006). These isomers correspond to the axial or equatorial orientation of the N-methyl substituent with the absolute minimum obtained for the rotation around the C6—O15 bond, which is characterized by an intramolecular O15H$\cdots$O4 hydrogen bond. In these structures, the tetrahydroazepine ring is in a chair conformation and the methoxy group is in a *trans* position with respect to the dihydrofuran ring.

The neutralization reactions of GALH$^+$ have been investigated according to

$$\mathrm{GALH}^+ + X = \mathrm{GALH}^+X. \qquad (1)$$

Energetics have been computed using the supermolecule approach

$$\Delta E = E(\mathrm{GALH}^+X) - E(\mathrm{GALH}^+) - E(X). \qquad (2)$$

These values have been calculated by taking into account the basis-set superposition error (BSSE) using the Counterpoise methodology with fragment relaxation (Boys & Bernardi, 1970; Xantheas, 1996).

Surface MEP (V_s) of the various species have been calculated at the MPWB1K level. The molecular surface was defined by the 0.001 e bohr^{-3} contour of the electronic density (Bader *et al.*, 1987). Patterns with positive ($V_s > 0$) and negative ($V_s < 0$) regions were respectively used to localize and analyze electrophilic and nucleophilic sites indicative of HBDs and HBAs. To probe in a more complete way the interaction potential of the O15H hydroxyl group, we have considered its three possible orientations. Hence, two supplementary conformers were added to the sample which correspond to *gauche* and *trans* orientations of the OH group with respect to the C5—C6 bond. For computational reasons, their examination has been limited to the complexes with water; a total of six conformers has therefore been studied in this part of the present work.

3. Results and discussion

3.1. Database analyses

The main hydrogen-bonding groups expected for galanthamine are: the hydroxyl, furanic and methoxy O15, O4 and O13 oxygen atoms as potential HBAs and the hydroxyl group as an HBD. To these strong HBAs and HBDs must be added weak HBA (π systems) and HBD (CH groups). Furthermore, the galanthamine structure allows us to examine the competition between intra- and intermolecular hydrogen bonding. In this section we analyze the HB interactions of galanthamine in AChE complexes and crystalline environments.

3.1.1. PDB. The five protein–ligand complexes related to galanthamine found in the PDB are 1DX6 (Greenblatt *et al.*, 1999), 1QTI (Bartolucci *et al.*, 2001), 1W4L, 1W6R and 1W76 entries (Greenblatt *et al.*, 2004). Recently, galanthamine has also been co-crystallized with the acetylcholine binding protein (Hansen & Taylor, 2007), a surrogate of the extracellular domain of nAChRs. However, the low resolution of this crystal structure (2.9 Å) and the binding of galanthamine in two different conformations in four of the subunits have led us to ignore this structure in our investigation. In 1DX6 and 1QTI, AChE have been co-crystallized with galanthamine whereas 1W4L, 1W6R and 1W76 entries involve co-crystals of AChE with bis-galanthaminium derivatives. Figs. 2(*a*) and (*b*) show respectively the specific interactions observed between

[1] Supplementary data for this paper, which gathers for the neutral, protonated and neutralized galanthamine isomers the total energies, optimized geometries and frequencies computed at the MPWB1K/6-31++G(d,p) level of theory, are available from the IUCr electronic archives (Reference: RY5017). Services for accessing these data are described at the back of the journal.

galanthamine and bis-galanthaminium derivatives with AChE based on the examples of the 1QTI and 1W6R structures. The cases of galanthamine and bis-galanthaminium derivatives have been considered separately owing to the significant changes of the galanthamine substructure: the iminium moiety in galanthaminium derivatives induces a flattening of the tetrahydroazepine ring. The two AChE–galanthamine complexes exhibit the same contacts with one noticeable exception: in the 1QTI structure the $N11H^+$ group of galanthamine interacts with a water molecule [$D(N^+\cdots O) = 3.30$ Å] not present in 1DX6. In fact, in the latter structure an O atom of a co-crystallized polyethyleneglycol (PEG) molecule lies strikingly at the same position to the water oxygen in 1QTI (Fig. 3*b*), giving rise to a strong $N11H^+\cdots O$ HB interaction [$D(N^+\cdots O) = 2.7$ Å]. The only difference in terms of HB interactions with AChE residues between the galanthamine and galanthaminium ligands appears limited to this interaction, which cannot occur with galanthaminium species.

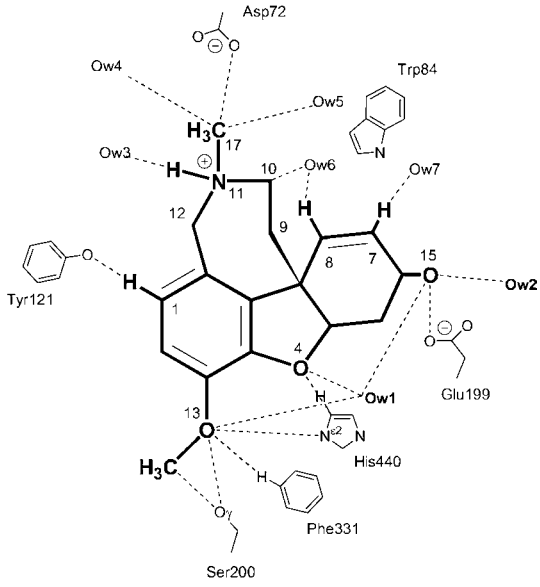

Figure 2
A representation of the specific intermolecular interactions formed by (*a*) galanthamine and (*b*) a bis-galanthaminium derivative in the binding sites of AChE (PDB entries 1QTI and 1W6R). Only the water molecules in direct contact with galanthamine are shown. Some relevant intermolecular distances (Å) corresponding to the mean of the interactions observed in 1DX6 and 1QTI for (*a*), and 1W6R, 1W4L and 1W76 for (*b*) are: (*a*) O15···$O^{\varepsilon1}$—Glu199 = 2.71; O15···O*w*1 = 2.84; O15···O*w*2 = 3.44; O4···O*w*1 = 3.07; O4···$C^{\delta2}$—His440 = 3.27; O13···O^{δ}—Ser200 = 3.10; O13···$N^{\varepsilon2}$—His440 = 3.59; O13···C^{ζ}—Phe331 = 3.31; O13···O*w*1 = 3.25; C14···O^{δ}—Ser200 = 3.24; N11···O*w*3 (O-PEG) = 3.00; C17···O*w*4 = 3.28; C17···O*w*5 = 3.23; C17···$O^{\delta2}$—Asp72 = 3.54; C8···O*w*6 = 3.24; C7···O*w*7 = 3.54; C9···Ce—Trp84 = 3.85. (*b*) O15···$O^{\varepsilon1}$—Glu199 = 2.69; O15···O*w*1 = 3.04; O15···O*w*2 = 3.52; O4···O*w*1 = 3.02; O4···$C^{\delta2}$—His440 = 3.36; O13···O^{δ}—Ser200 = 3.14; O13···$N^{\varepsilon2}$—His440 = 3.55; O13···C^{ζ}—Phe331 = 3.71; O13···O*w*1 = 2.69; C14···O^{δ}—Ser200 = 3.60; C17···O*w*4 = 3.39; C17···O*w*5 = 3.37; C17···$O^{\delta2}$—Asp72 = 3.53; C8···O*w*6 = 3.33; C7···O*w*7 = 3.57; C9···Ce-Trp84 = 3.84.

As shown in Fig. 2, the O15H group is always engaged in intermolecular hydrogen bonding with $O^{\varepsilon1}$ of the Glu199 carboxylate group. It is notable that the O15H group also appears to be engaged in hydrogen bonding with water molecules, one of them interacting with the O atom of the galanthamine dihydrofuran ring, O4. The O atom of the methoxy group (O13) also fulfils its HB potential since it interacts with the OH group of Ser200. On the basis of the HB distances, the strongest interaction is O15H···$^{-}$OOC-Glu199. The other specific interactions involve polarized methyl (C17) and methylene (C10 and C12) groups directly connected to the ammonium nitrogen. Indeed, these groups are expected to carry some of the positive charge of the ammonium nitrogen. These HB involve a charged residue $^{-}$OOC-Asp72 and water molecules (Fig. 2, *see below*). An aromatic HB is also noteworthy: it involves a positively polarized methylene group of galanthamine species (C9H) and the pyrrole ring of Trp84 (the average C9···Ce distance is 3.84 Å). This interaction appears to us worth mentioning owing to:

(i) its conservation in the five complexes;

(ii) its geometric parameters (the average C9H···Ce angle is *ca* 150°, the angle[2] between the pyrrole ring of Trp84 and the H atom being 90°);

(iii) the attested role of Trp84 in the binding of other AChE inhibitors (Silman *et al.*, 1998; Harel *et al.*, 1993; Quinn *et al.*, 2000).

Lastly, several weak HB involving aromatic CH groups of galanthamine or AChE residues are observed: $GALH^+$–C1H···(H)OPh–Tyr121, Phe331–CH···O13–$GALH^+$ and His440–CH···O4-$GALH^+$.

A closer examination of the HB interactions with water molecules also reveals interesting trends. The number of water molecules observed in the five PDB entries varies from four (1W76) to eight (1W6R). Among these, one (O*w*1, Figs. 2 and 3) is particularly remarkable since:

(i) it appears in interactions with three HB centers of galanthamine, O4, O13 and O15;

[2] The angle between the pyrrole ring of Trp 84 and the H atom of the C9H methylene group has been measured by defining the centroid of the pyrrole ring. The 90° value is the average of the five angles of the type ApCeH (Ap: pyrrole atom; Ce: centroid of the pyrrole ring).

Table 1
Displacement parameters (B factors, Å^2) in the five crystal structures of galanthamine–AChE complexes.

	1QTI	1DX6	1W6R	1W4L	1W76
Protein, all atoms	33	33	40	32	43
Water, all molecules	46	37	45	39	36
Active site, water molecules	29	26	33	30	33

(ii) it is strictly conserved in the five GAL-AChE complexes.

Fig. 3(*a*) shows the superposition of the various binding sites and illustrates this strong degree of conservation. Another water molecule (O*w*2, Figs. 2 and 3), which is at HB distances of the galanthamine O15 atom, is also observed in all the complexes. An unexpected observation is that the water molecules involved in weak hydrogen-bonding interactions (with polarized or ethylennic CH groups) are also among the most conserved. This is the case for the water molecules interacting with C17H, C7H and C8H groups.

In Table 1, average displacement parameters (B factors) for the five PDB entries are listed for all protein atoms, all water molecules and the active site water molecules. In all structures the active site water molecules exhibit values consistently lower than the average value for all protein atoms and for all water molecules. These water molecules thus have well defined positions. Furthermore, the water molecule at HB distances of O4, O13 and O15 galanthamine O atoms always has one of the lowest B factors.

It is of interest to compare the HB features of galanthamine pointed out through the present PDB analysis to the trends revealed by a recent thorough investigation on strong and weak HB in the protein–ligand interface (Panigrahi & Desiraju, 2007). Whereas for ligands the number of acceptors is generally around twice the number of donors, galanthamine presents a quasi-equivalent number of HB donors and acceptors (two and three groups, respectively, without considering the CH). Moreover, galanthamine has a number of furcated HB donors in the active site of AChE superior to the number of furcated acceptors (it is usually the opposite). Conversely, the water-mediated HBs of galanthamine with AChE are coherent with the conclusions drawn in the study of Panigrahi and Desiraju: there are more CH$\cdots$O*w* contacts than N$^+$H$\cdots$O*w* and OH$\cdots$O*w* ones.

Table 2
Geometric parameters of conventional HB observed in the crystal structures of galanthamine derivatives found in the CSD.

Refcode	D—H$\cdots$$A$	d (Å)	D (Å)	θ (°)	Φ (°)
(1) SIBHAM	O15H$\cdots$N11	2.03	2.92	148	120
(2) ECAFAQ	O15H$\cdots$O4†	2.29	2.93	122	100
	N11H$^+\cdots$Br$^-$	2.18	3.19	171	–
(3) GALAMI01	O15H$\cdots$O4†	2.17	2.89	129	100
(4) HUVVOJ	O15H$\cdots$O4†	2.38	3.01	121	98
	O15H$\cdots$O4	2.59	3.01	106	139
	O15H$\cdots$O13	2.19	3.05	145	121
	O15H$\cdots$O13	2.49	3.41	155	115
	O*w*H$\cdots$O15	1.80	2.75	161	120
	O*w*H$\cdots$O15	1.74	2.71	168	121
(5) HUVVOJ01	O15H$\cdots$O4†	2.58	3.01	107	97
	O15H$\cdots$O13	2.33	3.24	153	120
	O*w*H$\cdots$O15	1.77	2.74	171	119
(6) HUVVUP	O15H$\cdots$I$^-$	2.55	3.53	180	
	O15H$\cdots$I$^-$	2.57	3.55	180	
(7) NRGLNM	N11H$^+\cdots$O15	1.76	2.77	175	142
	N11H$^+\cdots$O15	1.83	2.81	163	135
	N11H$^+\cdots$Cl$^-$	2.15	3.11	158	–
	N11H$^+\cdots$Cl$^-$	2.10	3.04	154	–
	O15H$\cdots$Cl$^-$	2.07	3.05	173	–
	O15H$\cdots$O*w*	1.82	2.76	158	134
	O*w*H$\cdots$O4	2.04	2.94	150	111
	O*w*H$\cdots$O4	2.10	2.91	152	113
(8) RIWKOX	O15H$\cdots$O4†	2.13	2.87	130	101
	N11H$^+\cdots$Br$^-$	2.19	3.19	169	–
(9) YILTUI	O15H$\cdots$ClCH$_2$	2.26	3.08	140	133
	O15H$\cdots$ClCH$_2$	2.27	3.03	133	132

† Intramolecular O15H$\cdots$O4 HB.

3.1.2. CSD. To investigate more deeply the hydrogen-bonding properties of galanthamine, we have in a second step turned to the intermolecular interactions formed by the molecule in crystalline environments others than the receptor site. Among the 14 refcodes found in the CSD we have retained nine X-ray structures (Fig. 1). Neutral galanthamine corresponds to the first one, (1) (Carroll *et al.*, 1990), the remaining eight to charged derivatives, (2)–(9) (Hemetsberger *et al.*, 2004; Carroll *et al.*, 1990; Hirnschall *et al.*, 2003; Roques *et al.*, 1980; Peeters *et al.*, 1997; Matusch *et al.*, 1994). Tables 2 and 3 gather the geometric parameters

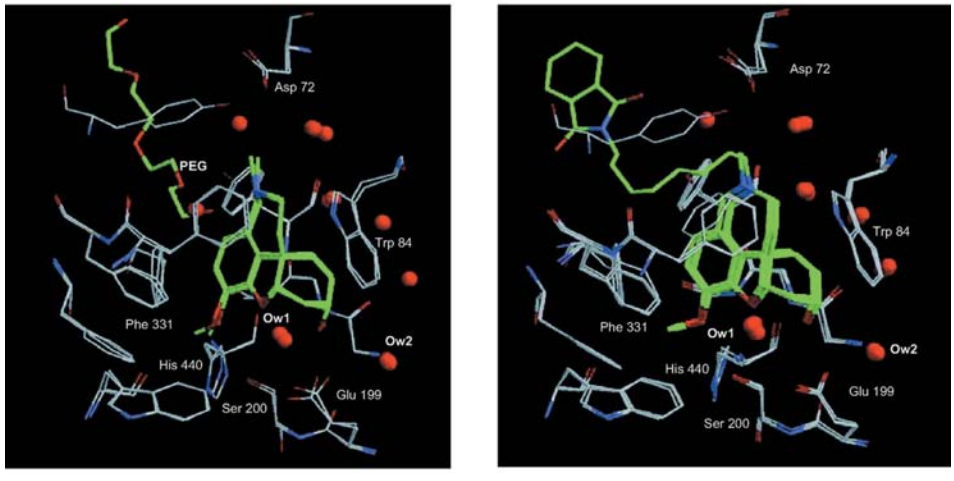

Figure 3
Superposition of AChE binding sites (*a*) 1QTI and 1DX6; (*b*) 1W6R, 1W4L and 1W76.

Table 3
Geometric parameters of the HB involving the CH groups of galanthamine derivatives observed in the CSD.

Refcode	D—H···A	d (Å)	D (Å)	θ (°)	Φ (°)
(2) ECAFAQ	C17H···O4	2.37	3.42	164	110
	C18′H···O13	2.42	3.45	158	117
(3) GALAMI01	C10H···O15	2.33	3.12	128	130
	C17H···O13	2.50	3.52	158	130
(4) HUVVOJ	C10H···O*w*	2.36	3.36	153	137
	C2H···O*w*	2.43	3.50	168	117
	C2H···O*w*	2.37	3.43	164	93
(5) HUVVOJ01	C2H···O*w*	2.46	3.53	169	92
(6) HUVVUP	C4*a*H···OC†	2.47	3.45	150	134
	C4*a*H···OC†	2.06	3.14	174	128
	C17H···O15	2.31	3.31	153	142
	C17H···O15	2.33	3.35	156	141
	C19H···O4	2.55	3.55	154	135
	C19H···O4	2.50	3.49	152	137
	C21H···O4	2.62	3.58	148	106
(7) NRGLNM	C8H···O15	2.51	3.59	175	136
	C12H···O*w*	2.51	3.50	152	133
	C12H···O*w*	2.22	3.29	170	127
	C14H···Cl^-	2.61	3.68	169	–
	C14H···Cl^-	2.62	3.68	168	–
(8) RIWKOX	C10H···O15	2.47	3.07	114	95
	C17H···O4	2.30	3.38	170	108
(9) YILTUI	C4*a*H···O13	2.62	3.62	153	94
	C9H···O13	2.58	3.52	144	104
	C12H···O13	2.52	3.44	142	121
	C12H···O13	2.60	3.49	139	117

† The OC group is a carbonyl of a cocrystallized dimethylformamide molecule.

of the HB interactions observed in the CSD and the nature of HBD and HBA involved. These interactions have been classified according to their expected HB strength: strong HBs are given first (Table 2) followed by weak ones (Table 3).

A total of 27 strong HBs are observed in the CSD. Table 2 shows that the O15H group appears as the main HB site of the molecule since it is involved in 21 HB, 16 as a HBD and five as a HBA. It is worth noting that the probability of forming an intramolecular HB (O15H···O4) in the solid state is significant (five observations on a total of 16 interactions involving the OH group as a HBD). The strongest interactions of Table 2 (d below 2.00 Å) involve the positive $N11H^+$ group, the O15H group and water molecules as the HBD, O15 and water O atoms as the HBA. The second group of interactions (from 2.00 to *ca* 2.60 Å) concerns most often the O15H group as the HBD and the O4 and O13 O atoms as the HBA. The remaining HB-type interactions involve *X*H groups engaged in interactions with halide ions (Cl^-, Br^- and I^-) of the crystal structures.

It is remarkable that the spatial proximity of the various O atoms of galanthamine can give rise to particular HB motifs: the O15H group can be involved in four-centered HBs, the H atom being located between the O4 of the same molecule (intramolecular HB) and the O4 and O13 atoms of another molecule (intermolecular HB). These interactions are observed in the HUVVOJ and HUVVOJ01 entries (Carroll *et al.*, 1990), which correspond to the low- and high-temperature forms of the same compound (Fig. 4). In the same way, it appears that the O4 and O13 atoms constitute an important HBA centre since, when the O15H group is not involved in HB with this site, the same role is fulfilled by water molecules. The distribution of OH donors around these atoms is illustrated in Fig. 5, which shows the superposition of the galanthamine subfragments containing the anisole (with O13) and dihydrofuran (with O4) rings (total of six observations). In four refcodes, the O15H group interacts only through intermolecular HB. They correspond to contacts with:

(i) Cl^- and I^- (Roques *et al.*, 1980; Hirnschall *et al.*, 2003; NRGLNM and HUVVUP refcodes, respectively);

(ii) the tetrahydroazepine N and the O atom of a water molecule in neutral galanthamine (Carroll *et al.*, 1990; SIBHAM entry);

(iii) the Cl atoms of the NCH_2Cl moiety (Matusch *et al.*, 1994; YILTUI refcode).

Table 2 shows that the intermolecular HB are significantly shorter than the intramolecular interactions. This observation is coherent with the much higher HBA strength of halide anions and tertiary amine compared with the anisole (O13) and dihydrofuran (O4) O atoms (Laurence & Berthelot, 2000).

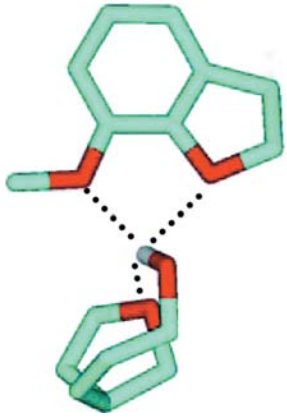

Figure 4
Four-centered HB observed in the HUVVOJ and HUVVOJ01 crystal structures (for the sake of clarity the H atoms not involved in the interactions are not represented).

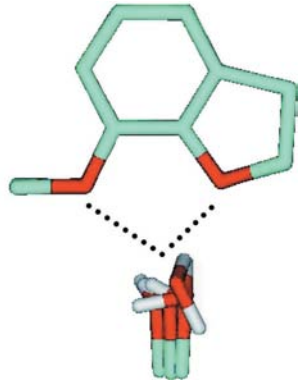

Figure 5
Superposition of galanthamine sub-fragments extracted from the CSD showing the distribution of OH donors around O4 and O13 atoms.

Table 4
Neutralization energies (ΔE in kJ/mol) of $GALH^+$ conformers and relative energies (δE in kJ/mol) of the corresponding $GALH^+X$ complexes.

	MPWB1K		MP2//MPWB1K	
Complex	ΔE†	δE‡	ΔE†	δE‡
$GALH^+Cl^-$				
ax§	−463.3	0.0	−468.4	0.0
eq§	−451.5	8.9	−458.7	8.9
$GALH^+H_2O$				
ax§	−54.5	0.0	−53.6	0.0
eq§	−53.2	−1.7	−53.6	−0.8
$GALH^+C_6H_6$				
ax§	−49.4	0.0	−62.1	0.0
eq§	−41.8	4.6	−61.8	−0.5

† Variation of the electronic energy for equation (2). ‡ Relative energy of the $GALH^+X$ complexes. § ax/eq: denotes the conformation of the *N*-methyl substituent in the galanthamine subfragment.

A total of 26 HBs involving CH groups as HBD are observed in the CSD (Table 3). More than half of these interactions involve the CH groups directly attached to the positive N atom (C10, C12 and C17). Indeed, these C atoms are expected to carry some of the positive charge of the ammonium nitrogen. Table 3 shows that the same HBA sites of the galanthamine molecule fulfill their potential: O4, O13 and O15 atoms. When this is not the case, the HB involves O atoms of water molecules or the halides counterions. The second type of HBD corresponds to unsaturated CH: among the four CH of galanthamine belonging to this category, only C2H and C8H interacts in such a way in four HBs. The third type illustrates the HB potential of CH directly linked to O atoms: C4*a* and C14. The remaining type of CH group does not belong to the galanthamine subfragment. Table 3 shows that the distances of HB interactions involving CH groups vary from 2.06 to 2.62 Å, the average being 2.43 Å. These results confirm that several CH groups of galanthamine appear as significant HB donors, which is important to consider in terms of potential HB sites.

On the whole, all these observations are consistent with the trends observed from the AChE–galanthamine complexes.

3.2. Theoretical calculations

In this section we first analyze some energetic and electrostatic properties computed for the neutralization of $GALH^+$ by various chemical species. Then we probe the interaction sites of galanthamine through the minima ($V_s < 0$) and maxima ($V_s > 0$) of the computed MEP.

3.2.1. Energetic properties of $GALH^+X$ complexes. Table 4 shows the results obtained at the MPWB1K and MP2//MPWB1K levels of theory for the complexation reaction of axial and equatorial *N*-methyl isomers of $GALH^+$ by a chloride anion, a water and a benzene molecule (X). Table 4 shows that the reaction energies are varying from −41.8 (X = C_6H_6) to −463.3 kJ mol^{-1} (X = Cl^-) at the MPWB1K level, the corresponding MP2//MPWB1K values being −61.8 to −468.4 kJ mol^{-1}.

The energies computed for the interaction of $GALH^+$ with the chlorine anion can be compared with the −500.3 and −499.5 kJ mol^{-1} values recently reported at the B3LYP/6-31+G(d,p) and MP2/6-31+G(d,p) levels by Davies *et al.* (2003) in their investigation of the $(CH_3)_3NH^+Cl^-$ ion pair. Our MPWB1K (MP2//MPWB1K) values, −463.3 (−468.4) and −451.5 (−458.7) kJ mol^{-1} for axial and equatorial isomers, appear a little smaller. These lower interaction energies probably find their origin in the greater size of the $GALH^+$ cation compared with $(CH_3)_3NH^+$ and to the associated increase of the positive charge delocalization. The binding energies of $GALH^+$ with water and benzene molecules can be compared with the experimental dissociation enthalpies, 60.7 and 66.5 kJ mol^{-1}, for $(CH_3)_3NH^+H_2O$ and $(CH_3)_3NH^+C_6H_6$ complexes, respectively (Mautner, 1984; Meot-Ner & Deakyne, 1985; Meot-Ner, 2005). The computed MPWB1K and MP2//MPWB1K values for the $GALH^+$ neutralization by water range from −53.2 to −54.5 kJ mol^{-1}, following the same trend as that observed for neutralization with Cl^-: the weaker interaction energies for $GALH^+$ compared with $(CH_3)_3NH^+$ illustrate the greater charge delocalization in the $GALH^+$ cation.

The interaction energies between $GALH^+$ and benzene appear very sensitive to the electron correlation treatment applied: the computed MPWB1K values for equatorial and axial isomers are −41.8 and −49.4 kJ mol^{-1}, respectively, while the corresponding MP2//MPWB1K values are −61.8 and −62.1 kJ mol^{-1}. Furthermore, the BSSE at the MP2//MPWB1K level of theory represents up to 23% of the interaction energy before counterpoise correction. To determine precisely the binding energies of $GALH^+$ with the benzene molecule, further calculations have been made using the local MP2 (LMP2) method (Pulay & Saeboe, 1986; Saebo & Pulay, 1993), which eliminates BSSE to a large extent (Saebo *et al.*, 1993; Hampel & Werner, 1996; Pedulla *et al.*, 1996), in conjunction with a large basis set, namely aug-cc-pVTZ(-f). The calculated LMP2//MPWB1K binding energies for the axial and equatorial isomers are −55.0 and −53.7 kJ mol^{-1}, the remaining BSSE being neglected as it is estimated to a few tenths of kJ mol^{-1}.[3] They compare well with the experimental dissociation enthalpy of 66.5 kJ mol^{-1} for the complex between trimethylammonium and benzene, the difference being in agreement with the previously revealed trend on the variation of size between the two cations and the associated effects. On the whole, the binding energies computed for the two isomers of $GALH^+$ within the various chemical species are close, suggesting comparable reactivities, and follow the sequence: $GALH^+Cl^- > GALH^+C_6H_6 \simeq GALH^+H_2O$.

3.2.2. Molecular electrostatic potential of $GALH^+X$ complexes. It is now well established that considerable insight into non-covalent interactions and especially hydrogen

[3] The BSSE is always lower at the LMP2 level of theory than at the HF one and, with a large basis set, the LMP2 BSSE is expected to be smaller than half the HF BSSE obtained with the same basis set (Pedulla *et al.*, 1996; Schuetz *et al.*, 1998; Hill *et al.*, 2006). At HF/aug-cc-pVTZ(-f)//MPWB1K/6-31++G(d,p), the BSSE related to the interaction energies between C_6H_6 and the axial and equatorial $GALH^+$ isomers is −1.6 and −1.7 kJ mol^{-1}, respectively.

Table 5
Minima of the electrostatic potential ($V_{s,min}$, kJ mol^{-1}) computed on the molecular surfaces of various species of galanthamine at the MPWB1K level.

Complex	O15	O15—O4—O13	O4—O13	N11	Benzene ring
GAL					
ax†	−172	–	−148	−113	−66
eq†	−174	–	−151	−133	−68
$GALH^+Cl^-$					
ax†	−141	–	−102	–	−14
eq†	−155	–	−131	–	−31
$GALH^+H_2O$					
ax1†‡	14	–	83	–	199
ax2†‡§	–	−4	–	–	179
ax3†¶	29	–	50	–	174
eq1†‡	19	–	96	–	213
eq2†§	–	6	–	–	196
eq3†¶	44	–	66	–	190
$GALH^+C_6H_6$					
ax†	15	–	82	–	200
eq†	17	–	90	–	205
$GALH^+$					
ax†	24	–	97	–	217
eq†	24	–	97	–	216

† ax/eq: denotes the conformation of the *N*-methyl substituent in the galanthamine subfragment. ‡ Number 1 denotes the $GALH^+$ conformation with intramolecular O15H···O4 HB. § Number 2 denotes the $GALH^+$ conformation with a *trans* orientation of the O15H group with respect to the C5—C6 bond. ¶ Number 3 denotes the $GALH^+$ conformation with a *gauche* orientation of the O15H group with respect to the C5—C6 bond.

Table 6
Maxima of the electrostatic potential ($V_{s,max}$, kJ mol^{-1}) computed on the molecular surfaces of various species of galanthamine at the MPWB1K level.

Complex	$N11H^+$	O15H	C10H—C12H—C17H	C1H—C2H	C14H
GAL					
ax†	–	–	52–73	67–87	67–70
eq†	–	–	39–69	68–85	66–67
$GALH^+Cl^-$					
ax†	–	–	93–127	104–127	96–102
eq†	–	–	96–155	103	75–80
$GALH^+H_2O$					
ax1†‡	478	–	378–478	311	246–260
ax2†§	471	378	368–471	296	231–245
ax3†¶	467	360	367–467	297	234–245
eq1†‡	482	–	390–482	328	257–273
eq2†§	471	383	382–471	313	245–259
eq3†¶	466	377	382–466	314	250–262
$GALH^+C_6H_6$					
ax†	–	–	377–424	82	–
eq†	–	–	301–444	90	–
$GALH^+$					
ax†	598	–	405–417	326	272
eq†	576	–	417–475	325	270

† ax/eq: denotes the conformation of the *N*-methyl substituent in the galanthamine subfragment ‡ Number 1 denotes the $GALH^+$ conformation with intramolecular O15H···O4 HB. § Number 2 denotes the $GALH^+$ conformation with a *trans* orientation of the O15H group with respect to the C5—C6 bond. ¶ Number 3 denotes the $GALH^+$ conformation with a *gauche* orientation of the O15H group with respect to the C5—C6 bond.

bonding can be obtained from the analysis of the minima ($V_{s,min}$) and maxima ($V_{s,max}$) of the electrostatic potential computed on the van der Waals surface of molecules (Politzer & Murray, 2002; Hunter, 2004). The usefulness of these parameters can be illustrated by family-dependent quantitative relationships established between $V_{s,min}$ and experimental values of HB accepting strength for several organic functionalities (Brinck, 1998; Le Questel *et al.*, 2000; Graton, Berthelot *et al.*, 2003). In the present work we have chosen these parameters to locate HBA and HBD in various $GALH^+X$ complexes. For the sake of comparison, the electrostatic potential has been computed for the neutral and protonated forms of galanthamine. Our objectives are:

(i) to identify the main HB interaction sites of the various complexes;

(ii) to probe the influence of the *X* chemical species on the minima and maxima of the electrostatic potential.

Tables 5 and 6 present the $V_{s,min}$ and $V_{s,max}$ values computed at the MPWB1K level for the various complexes, while Figs. 6(*a*)–(*c*) illustrate their location on selected $GALH^+H_2O$ complexes.

Table 5 shows drastic changes in the values of the local minima from neutral to the cationic form of galanthamine. For example, the value corresponding to the site located at the O4–O13 atoms ranges from −151 in neutral galanthamine (GAL) to +97 kJ mol^{-1} in the protonated form ($GALH^+$). Of course, these variations reflect the influence of the positive charge, which induce a depletion of the electronic density on the whole molecule. In the present work we will not discuss such absolute values that must be considered with caution owing to the important variations in the chemical form of galanthamine, but will comment on the relative evolution of these parameters in the various species investigated. The behavior of the $GALH^+Cl^-$ complex is compared with neutral galanthamine (the values are from 20 to *ca* 45 kJ mol^{-1} less negative), a trend which reflects the strong interaction with the chloride anion and the resulting important neutralization of the positive charge. Conversely, the values computed for the $GALH^+H_2O$ and $GALH^+C_6H_6$ species are very close to the protonated form $GALH^+$. Indeed, in interaction with water and benzene the galanthamine fragment keeps most of the positive charge and must therefore have lost a significant amount of its nucleophilic character. Whatever the chemical species of galanthamine, the main nucleophilic sites (potential HBA) are the O atoms. Analysis of the MEP minima data reveal distinct features in these interaction sites according to the existence of an intramolecular O15H···O4 HB. When this interaction is present, two nucleophilic zones are observed which correspond to the electron pairs of O4–O13 (mainly O13 since O4 is engaged in intramolecular HB) and O15 atoms (Fig. 6*a*). Conversely, for a *trans* orientation of the hydroxyl group only one enhanced nucleophilic area is visible for the three O atoms (Fig. 6*b*). This result is in agreement with the motif observed in the binding site of AChE in which a strictly conserved water molecule is at HB distances of the O4, O13 and O15 atoms. Lastly, the differences between the axial and equatorial conformers do not appear significant. Nevertheless, in the case of the $GALH^+Cl^-$ complex the equatorial isomer appears more nucleophilic (more negative values from 15 to 30 kJ mol^{-1}), and in the case of the $GALH^+H_2O$ complex conversely the axial isomer comes out slightly more nucleophilic (on average of 13 kJ mol^{-1}).

The MEP maxima reported in Table 6 show strong variations between the various galanthamine species. As expected, the most electrophilic species appears as $GALH^+$ and the weakest one is neutral galanthamine: the HBD potential is raised from GAL to $GALH^+$. In agreement with the trends revealed from the MEP minima analysis, the behaviour of the $GALH^+Cl^-$ complex is close to that of GAL, whereas the $GALH^+H_2O$ and $GALH^+C_6H_6$ species behave rather like the protonated form, $GALH^+$. The main electrophilic sites of the various species correspond to:

(i) the $N11H^+$ hydrogen (it is remarkable that despite the interaction with a water molecule, the electrophilic character of this zone remains available for further interactions);

(ii) the O15H hydrogen for the conformations without the intramolecular O15H···O4 HB;

(iii) the H atoms carried by the C atoms (C10, C12 and C17) directly linked to the positive nitrogen;

(iv) the H atoms of the aromatic ring C1 and C2 and of the methoxy group C14 atom (Fig. 6*c*).

The computed data in the isolated state agree well with the experimental observations in crystalline environments, as well as in the AChE binding site in organic crystal structures. Finally, while significant differences are observed inside most of the species between the various conformers, Table 6 shows that the strongest variations are observed for the CH groups carried by the ammonium nitrogen (directly influenced by the degree of neutralization of the positive charge). In all the species, these groups are more electrophilic for the equatorial isomer than for the axial one. Moreover, galanthamine neutralized by water appear more potent, compared with the complexes with benzene, for binding with AChE. Indeed, significant electrophilic sites are more numerous in the water complexes. These remarks are important owing to the well established role of water molecules and aromatic residues in the inhibitor–AChE binding process.

On the whole, this analysis of computed energetic and electrostatic properties of $GALH^+X$ complexes shows very distinct features depending on the nature of *X*.

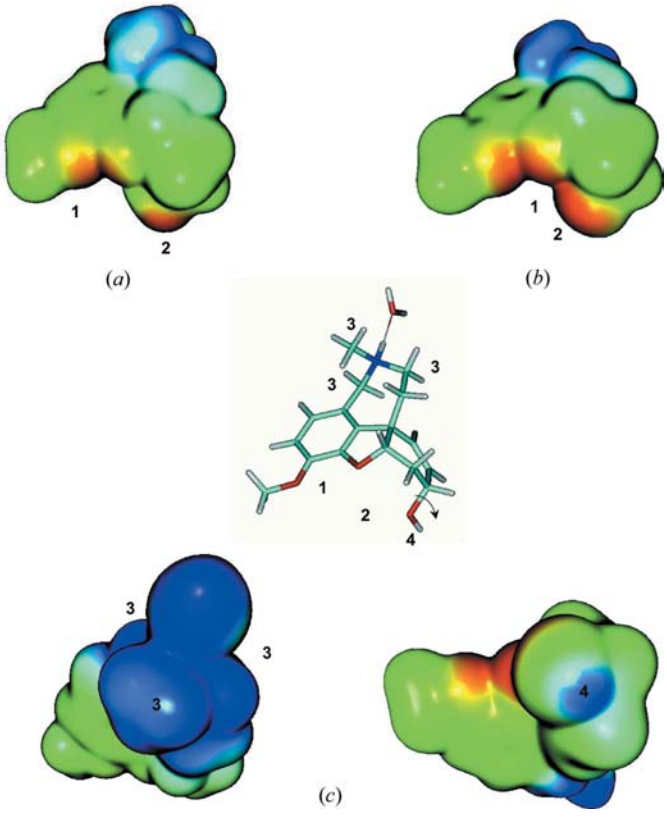

Figure 6
MEP extrema of the $GALH^+H_2O$ complex: (*a*) minima for the $GALH^+$ conformation with intramolecular O15H···O4 HB; (*b*) minima for the $GALH^+$ conformation with a *trans* orientation of the O15H group with respect to the C5—C6 bond; (*c*) maxima for the $GALH^+$ conformation with a *trans* orientation of the O15H group with respect to the C5—C6 bond (positive values are shown in blue, negative values in red).

4. Conclusions

From crystallographic observations in the CSD and PDB databases, and gas-phase *ab initio* and DFT calculations on various species of galanthamine we have shown that:

(i) The main HBA sites of the molecule are the O4, O13 and O15 atoms.

(ii) The spatial proximity of these O atoms can give rise to multi-centered HB interactions such as those observed in the AChE binding site and the CSD. These observed preferences are rationalized through the localization of the MEP minima on the molecular surface.

(iii) The occurrence of multicentered HB interactions is sensitive to the conformation of galanthamine, especially the existence of an intramolecular O15H···O4 HB.

(iv) As far as the HBD properties are concerned, the most important sites of galanthamine are the $N11H^+$ and O15H groups, but the contacts established with CH donors are more numerous. These 'unconventional' HBD appear therefore as inevitable interaction sites during the molecular recognition processes involving galanthamine. Among these groups, the most electrophilic are the CH groups in the vicinity of the ammonium nitrogen. The analysis of the MEP maxima is in good agreement with the interactions of galanthamine in crystalline environments.

(v) The molecular recognition properties of the galanthamine fragment depend strongly on the neutralization degree of the $N11H^+$ positive charge.

The present work provides important information on the molecular recognition properties of galanthamine that should help to rationalize the observed behaviour of this anti-Alzheimer agent and its derivatives during the transport and docking processes to their receptors.

The authors gratefully acknowledge the IDRIS (Institut du Développement et des Ressources en Informatique), the CINES (Centre Informatique National de l'Enseignement Supérieur) and the CCIPL (Centre de Calcul Intensif des Pays de la Loire) for grants of computer time. SK and EHSB would like to thank the AUF (Agence Universitaire de la Francophonie) for financial support and the LCOS (Laboratoire de

Chimie Organique Structurale) of Abidjan Cocody University for its help.

References

Allen, F. H. (2002). *Acta Cryst.* B**58**, 380–388.

Allen, F. H., Kennard, O., Watson, D. G., Brammer, L., Orpen, A. G. & Taylor, R. (1987). *J. Chem. Soc. Perkin Trans. 2*, pp. S1–S19.

Bader, R. F. W., Carroll, M. T., Cheeseman, J. R. & Chang, C. (1987). *J. Am. Chem. Soc.* **109**, 7968–7979.

Bartolucci, C., Perola, E., Pilger, C., Fels, G. & Lamba, D. (2001). *Proteins Struct. Funct. Genet.* **42**, 182–191.

Berman, H. M., Westbrook, J., Feng, Z., Gilliland, G., Bhat, T. N., Weissig, H., Shindyalov, I. N. & Bourne, P. E. (2000). *Nucl. Acids Res.* **28**, 235–242.

Boys, S. F. & Bernardi, F. (1970). *Mol. Phys.* **19**, 553–566.

Brinck, T. (1998). *Theor. Comput. Chem.* **5**, 51–93.

Bruno, I. J., Cole, J. C., Edgington, P. R., Kessler, M., Macrae, C. F., McCabe, P., Pearson, J. & Taylor, R. (2002). *Acta Cryst.* B**58**, 389–397.

Carroll, P., Furst, G. T., Han, S. Y. & Joullie, M. (1990). *Bull. Soc. Chim. Fr.* pp. 769–780.

Davies, A. S., George, W. O. & Howard, S. T. (2003). *Phys. Chem. Chem. Phys.* **5**, 4533–4540.

Delano, W. L. (2004). *PyMOL*. DeLano Scientific LLC; http://www.pymol.org.

Desiraju, G. & Steiner, T. (1999). *The Weak Hydrogen Bond: Applications to Structural Chemistry and Biology*. Oxford University Press.

Frisch, M. J. *et al.* (2004). *GAUSSIAN*03, Revision C.02. Gaussian Inc., Wallingford, CT, USA.

Geerts, H., Finkel, L., Carr, R. & Spiros, A. (2002). *J. Neural Transm. Suppl.* **62**, 203–216.

Graton, J., Berthelot, M., Gal, J.-F., Laurence, C., Lebreton, J., Le Questel, J.-Y., Maria, P.-C. & Robins, R. (2003). *J. Org. Chem.* **68**, 8208–8221.

Graton, J., van Mourik, T. & Price, S. L. (2003). *J. Am. Chem. Soc.* **125**, 5988–5997.

Greenblatt, H. M., Guillou, C., Guenard, D., Argaman, A., Botti, S., Badet, B., Thal, C., Silman, I. & Sussman, J. L. (2004). *J. Am. Chem. Soc.* **126**, 15405–15411.

Greenblatt, H. M., Kryger, G., Lewis, T., Silman, I. & Sussman, J. L. (1999). *FEBS Lett.* **463**, 321–326.

Hampel, C. & Werner, H.-J. (1996). *J. Chem. Phys.* **104**, 6286–6297.

Hansen, S. B. & Taylor, P. (2007). *J. Mol. Biol.* **369**, 895–901.

Harel, M., Schalk, I., Ehret-Sabatier, L., Bouet, F., Goeldner, M., Hirth, C., Axelsen, P. H., Silman, I. & Sussman, J. L. (1993). *Proc. Natl. Acad. Sci. USA*, **90**, 9031–9035.

Hemetsberger, M., Treu, M., Jordis, U., Mereiter, K., Hametner, C. & Froehlich, J. (2004). *Monatsh. Chem.* **135**, 1275–1287.

Hendlich, M., Bergner, A., Gunther, J. & Klebe, G. (2003). *J. Mol. Biol.* **326**, 607–620.

Hill, J. G., Platts, J. A. & Werner, H.-J. (2006). *Phys. Chem. Chem. Phys.* **8**, 4072–4078.

Hirnschall, M., Treu, M., Mereiter, K., Hametner, C., Frohlich, J. & Jordis, U. (2003). *Tetrahedron Asym.* **14**, 675–681.

Hunter, C. A. (2004). *Angew. Chem. Int. Ed.* **43**, 5310–5324.

Iorga, B., Herlem, D., Barre, E. & Guillou, C. (2006). *J. Mol. Model.* **12**, 366–372.

Koellner, G., Kryger, G., Millard, C. B., Silman, I., Sussman, J. L. & Steiner, T. (2000). *J. Mol. Biol.* **296**, 713–735.

Koellner, G., Steiner, T., Millard, C. B., Silman, I. & Sussman, J. L. (2002). *J. Mol. Biol.* **320**, 721–725.

Kone, S., Galland, N., Graton, J., Illien, B., Laurence, C., Guillou, C. & Le Questel, J.-Y. (2006). *Chem. Phys.* **328**, 307–317.

Laurence, C. & Berthelot, M. (2000). *Perspect. Drug Discovery Des.* **18**, 39–60.

Le Questel, J.-Y., Berthelot, M. & Laurence, C. (2000). *J. Phys. Org. Chem.* **13**, 347–358.

Lilienfeld, S. (2002). *CNS Drug Rev.* **8**, 159–176.

Matusch, R., Kreh, M. & Mueller, U. (1994). *Helv. Chim. Acta*, **77**, 1611–1615.

Mautner, M. (1984). *J. Am. Chem. Soc.* **106**, 257–264.

Meot-Ner, M. (2005). *Chem. Rev.* **105**, 213–284.

Meot-Ner, M. & Deakyne, C. A. (1985). *J. Am. Chem. Soc.* **107**, 474–479.

Panigrahi, S. K. & Desiraju, G. R. (2007). *Proteins Struct. Funct. Bioinf.* **67**, 128–141.

Pedulla, J. M., Vila, F. & Jordan, K. D. (1996). *J. Chem. Phys.* **105**, 11091–11099.

Peeters, O. M., Blaton, N. M. & De Ranter, C. J. (1997). *Acta Cryst.* C**53**, 1284–1286.

Politzer, P. & Murray, J. S. (2002). *Theor. Chem. Acc.* **108**, 134–142.

Proskurnina, N. F. & Yakovleva, A. P. (1952). *Zh. Obshch. Khim.* **22**, 1941–1944.

Pulay, P. & Saeboe, S. (1986). *Theor. Chim. Acta*, **69**, 357–368.

Quinn, D. M., Feaster, S. R., Nair, H. K., Baker, N. A., Radic, Z. & Taylor, P. (2000). *J. Am. Chem. Soc.* **122**, 2975–2980.

Roques, R., Rossi, J. C., Declercq, J. P. & Germain, G. (1980). *Acta Cryst.* B**36**, 1589–1593.

Saebo, S. & Pulay, P. (1993). *Annu. Rev. Phys. Chem.* **44**, 213–236.

Saebo, S., Tong, W. & Pulay, P. (1993). *J. Chem. Phys.* **98**, 2170–2175.

Santos, M. D., Alkondon, M., Pereira, E. F. R., Aracava, Y., Eisenberg, H. M., Maelicke, A. & Albuquerque, E. X. (2002). *Mol. Pharmacol.* **61**, 1222–1234.

Schrödinger (2005). *Jaguar*, Version 6.0. Schrödinger LLC, New York.

Schuetz, M., Rauhut, G. & Werner, H.-J. (1998). *J. Phys. Chem. A*, **102**, 5997–6003.

Silman, I., Harel, M., Raves, M. & Sussman, J. L. (1998). *Adv. Behav. Biol.* **49**, 523–530.

Sramek, J. J., Frackiewicz, E. J. & Cutler, N. R. (2000). *Expert Opin. Investig. Drugs*, **9**, 2393–2402.

Weinstock, M. (1999). *CNS Drugs*, **12**, 307–323.

Wlodek, S. T., Clark, T. W., Scott, L. R. & McCammon, J. A. (1997). *J. Am. Chem. Soc.* **119**, 9513–9522.

Xantheas, S. S. (1996). *J. Chem. Phys.* **104**, 8821–8824.

Zhao, Y., Tishchenko, O. & Truhlar, D. G. (2005). *J. Phys. Chem. B*, **109**, 19046–19051.

Zhao, Y. & Truhlar, D. G. (2004). *J. Phys. Chem. A*, **108**, 6908–6918.

Zhao, Y. & Truhlar, D. G. (2005*a*). *J. Chem. Theory Comput.* **1**, 415–432.

Zhao, Y. & Truhlar, D. G. (2005*b*). *Phys. Chem. Chem. Phys.* **7**, 2701–2705.